Published March, 2003

Using the Dual-Pathway Parallel Conductance Model to Determine How Different Soil Properties Influence Conductivity Survey Data

S. M. Lesch* and D. L. Corwin

ABSTRACT

The correlation structure between apparent soil electrical conductivity (EC_a) and various soil properties can often appear radically dissimilar in different field surveys. Ideally, some type of methodology for survey data validation should be developed that can predict the expected correlation structure between EC_a survey data and various soil properties, given information about the soil properties themselves. In this paper, we review an existing model for EC_a and hypothesize that this model can be used to accurately predict the expected correlation structure between EC_a data and multiple soil properties of interest (such as soil salinity, saturation-paste percentage, and soil water content). Our objective is twofold: (i) to demonstrate how this model can be employed to produce the expected correlation structure and (ii) to extend this EC_a model to handle survey data collected under low water content situations by dynamically adjusting the model's assumed water content function. This adjustment can be estimated using acquired EC_a signal and soil sample data, and its statistical significance can be determined for each specific survey situation. We demonstrate both of these techniques using acquired electromagnetic induction signal data and measured soil properties of interest from 12 different field salinity surveys performed in California and Colorado and in Alberta, Canada. Results from these 12 surveys suggest that the ordinary model is able to accurately predict the expected correlation structure between conductivity and soil property when the water content is near field capacity and that the dynamically adjusted model is able to substantially improve the accuracy of the predicted correlation structure when the water content is significantly below field capacity.

Within the last decade, the collection of spatial soil electrical conductivity data has played an increasingly important role in precision-farming research. The collection of such data typically focuses on the assessment of spatial variation in one or more soil properties, as inferred by the observed spatial variation in the EC_a survey data. Depending on the specific survey application, the *target* variable of interest is usually soil salinity, soil texture, and/or soil water content although sometimes information about additional soil properties may also be ascertained (i.e., organic matter, clay content, sodium adsorption ratio, B, etc.).

There are numerous technical articles that document the relationships between EC_a and various soil physicochemical properties, including soil salinity (Williams and Baker, 1982; Rhoades et al., 1989; Slavich and Petterson, 1990; Hendrickx et al., 1992; Rhoades, 1992, 1996a, 1996b; Lesch et al., 1995a;), clay content (Williams and Hoey, 1987; Cook et al., 1992), depth to clay layers (Doolittle et al., 1994), nutrient status (Suddeth et al., 1995), sand deposition (Kitchen et al., 1996), and moisture content (Kachanoski et al., 1988; Sheets and Hendrickx, 1995). Additionally, there are articles documenting the use of conductivity survey information for yield mapping (Jaynes et al., 1995), determining salt loading and field irrigation efficiency (Rhoades et al., 1997), estimating leaching and salt loading (Corwin et al., 1996, 1999; Rhoades et al., 1999a), estimating deep drainage (Triantafilis et al., 1998), and designing optimal salinity sampling and monitoring strategies (Lesch et al., 1995b, 1998). A comprehensive review of the various methods of soil salinity assessment via electrical conductivity measurements is given in Rhoades et al. (1999b) and Hendrickx and Kachanoski (2002), and the use of conductivity survey information for precision-farming applications is discussed in Rhoades et al. (1999b) and Corwin and Lesch (2003).

Particular interest in any given EC_a survey is often focused toward ensuring that the acquired EC_a data correlate well with the prespecified target soil variable. For example, in a soil salinity survey, one generally attempts to maximize the correlation between salinity and EC_a by minimizing the corresponding variation in soil texture and water content using different area substratification schemes (for minimizing texture variation) or timing strategies (for minimizing water content variation). In spite of these efforts, considerable variation is sometimes observed in the observed correlation between salinity and EC_a. Indeed, as indicated by the above-mentioned references, EC_a often correlates to some degree with several different soil properties. Furthermore, the strength of these observed correlation estimates can vary widely from one survey to the next. To a certain extent, these apparent inconsistencies have resulted in some unfortunate confusion in the general soils literature with respect to how well different soil properties are expected to correlate with EC_a data.

Rhoades et al. (1989) developed a model for EC_a based on data collected across the arid southwestern United States. This model was developed to predict the effects that soil salinity, soil texture, bulk density (ρ_b),

USDA-ARS George E. Brown, Jr., Salinity Lab., 450 West Big Springs Rd., Riverside, CA 92507-4617. Received 29 Mar. 2002. *Corresponding author (slesch@ussl.ars.usda.gov).

Published in Agron. J. 95:365–379 (2003).

Abbreviations: $CalcEC_a$, calculated soil electrical conductivity; DPPC, dual-pathway parallel conductance (model); Dy-DPPC, dynamic water content partitioning (model); EC_a, apparent soil electrical conductivity; EC_e, electrical conductivity of the saturated soil extract; EC_{wc}, specific electrical conductivity of the continuous soil water phase; EC_{ws}, specific electrical conductivity of the series-coupled soil water phase; EM, electromagnetic induction; EM_{avg}, average electromagnetic induction; SP, saturation percentage; Θ_g, gravimetric soil water content; Θ_w, volumetric soil water content; Θ_{wc}, volumetric soil water content in the continuous liquid pathway; Θ_{ws}, volumetric soil water content in the series-coupled pathway; ρ_b, bulk density; Ω_{wc}, adjusted volumetric soil water content of continuous liquid pathway; Ω_{ws}, adjusted volumetric soil water content of series-coupled pathway.

and soil water content have on soil conductivity signal data. This model was originally intended to be used primarily for the prediction of soil salinity [expressed as electrical conductivity of the saturated soil extract (EC_e)], given measurements of both the soil conductivity and remaining primary soil properties (texture, ρ_b, and water content). However, because this model is capable of simultaneously describing multiple soil property effects, we hypothesized that it might be successfully used to explain the diverse variation in observed EC_a–soil property correlation estimates.

The purpose of this paper is twofold. First, we describe how the EC_a model developed by Rhoades et al. (1989) can be used to accurately predict the expected correlation structure between EC_a data and multiple soil properties of interest for an arbitrary survey process. The methodology that is developed to predict this correlation structure serves both as a useful procedure for survey data validation and, in a broader sense, a quantitative technique for understanding how different soil properties influence (and hence correlate with) the acquired EC_a data. Furthermore, this technique is shown to be generally reliable, provided the relative soil water content (across the survey area) is not significantly below field capacity.

Second, we show how this EC_a model can be extended to handle survey data collected under low water content situations by dynamically adjusting the assumed water content partitioning function specified in the model. This partitioning function can be estimated using acquired EC_a survey and soil sample data, and its statistical significance can be determined for each specific survey situation. Under especially low water content situations, this adjustment can result in a substantial improvement in the accuracy of the predicted correlation structure. We demonstrate these results using data from 12 different salinity surveys performed over the last 10 yr in California and Colorado and in Alberta, Canada.

THEORY

In the following section, a model for EC_a, originally developed by Rhoades et al. (1989), is reviewed. This model is then incorporated into a data validation procedure designed to be performed on measured EC_a and soil sample survey data. This procedure produces the expected correlation levels between the acquired conductivity data and measured soil properties of interest and hence simultaneously addresses the expected EC_a–soil variable question raised in the introduction. Finally, the original model introduced by Rhoades and his colleagues is extended to handle data collected under low water content survey conditions.

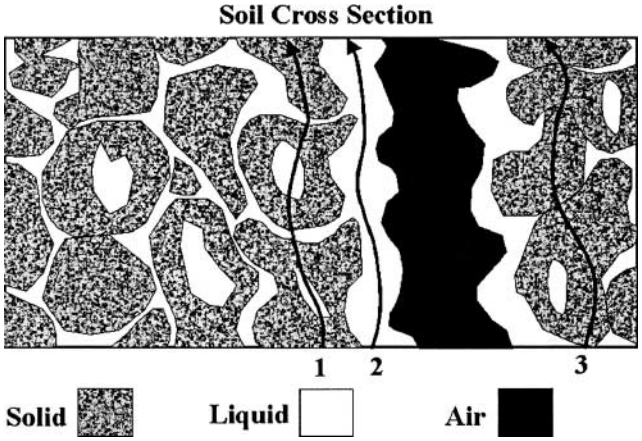

Fig. 1. The three theoretical current-flow pathways within a mixed soil–water system, as originally described by Rhoades et al. (1989): (1) the series-coupled pathway, (2) the continuous liquid pathway, and (3) indurated solid phase pathway.

A Review of the Dual-Pathway Parallel Conductance Model

Rhoades et al. (1989) introduced a model describing the expected electrical conductivity of a mixed soil–water system, based on the partitioning of the system into three separate current-flow pathways acting in parallel. These pathways are illustrated in Fig. 1 and are as follows: (i) a conductance pathway traveling through alternating layers of soil particles and soil solution, (ii) a conductance pathway traveling through the continuous soil solution, and (iii) a conductance pathway traveling through or along the surface of soil particles in direct and continuous contact. Conceptually, the first pathway can be thought of as a solid-liquid, series-coupled element. Likewise, the second and third pathways represent continuous liquid and solid elements, respectively.

Mathematically, this model can be written as:

$$EC_a = \left[\frac{(\Theta_{ss} + \Theta_{ws})^2 \times EC_{ws} \times EC_{ss}}{(\Theta_{ss} \times EC_{ws}) + (\Theta_{ws} \times EC_{ss})}\right] + (\Theta_{sc} \times EC_{sc}) + (\Theta_{wc} \times EC_{wc}) \quad [1]$$

where

Θ_{ws} = volumetric soil water content in the series-coupled pathway
Θ_{wc} = volumetric soil water content in the continuous liquid pathway
Θ_{ss} = volumetric content of the surface conductance soil phase
Θ_{sc} = volumetric content of indurated solid phase
EC_{ws} = specific electrical conductivity of the series-coupled soil water phase
EC_{wc} = specific electrical conductivity of the continuous water phase
EC_{ss} = electrical conductivity of the surface conductance soil phase
EC_{sc} = electrical conductivity of the indurated soil phase (Rhoades et al., 1999b)

As reported by Rhoades et al. (1989), experimental work demonstrated that the conductance contributed by the indurated solid phase was negligible, i.e.,

$$\Theta_{sc} \times EC_{sc} \approx 0$$

Additionally, because volumetric soil water content (Θ_w) = $\Theta_{ws} + \Theta_{wc}$, Eq. [1] can be reduced to:

$$EC_a = \left[\frac{(\Theta_{ss} + \Theta_{ws})^2 \times EC_{ws} \times EC_{ss}}{(\Theta_{ss} \times EC_{ws}) + (\Theta_{ws} \times EC_{ss})}\right] +$$

$$(\Theta_w - \Theta_{ws}) \times EC_{wc} \quad [2]$$

which essentially represents a dual-pathway parallel conductance (DPPC) current flow system. Hence, Eq. [2] will be hereafter referred to as the DPPC model.

An important relationship inherent in the DPPC model is that the combined soil electrical conductivity (EC_w) of both the continuous solution (EC_{wc}) and soil–water interface (EC_{ws}) may be expressed as:

$$\Theta_w \times EC_w = (\Theta_{ws} \times EC_{ws}) + (\Theta_w \times EC_{wc}) \quad [3]$$

Additionally, the expected relationship between EC_w and soil salinity (EC_e) is assumed to be

$$\Theta_w \times EC_w \approx (EC_e \times \rho_b \times SP)/100 \quad [4]$$

where SP represents the saturation percentage of the soil. This latter relationship is only strictly valid for chloride-salt systems. However, this approximation has been found to work reasonably well for most mixed chemistry systems, as shown by Rhoades et al. (1989, 1999b). Solving Eq. [3] for EC_w yields

$$EC_w = \alpha \times EC_{ws} + (1 - \alpha) \times EC_{wc} \quad [5]$$

where $\alpha = \Theta_{ws}/\Theta_w$. However, in Rhoades et al. (1989), an additional assumption of solution conductivity *equilibrium* was made, i.e., $EC_w = EC_{ws} = EC_{wc}$. Rhoades and colleagues argued that this assumption should be reasonable, provided the field water content was at or near field capacity.

Given the additional assumption of equilibrium, the DPPC model further simplifies to:

$$EC_a = \left[\frac{(\Theta_s + \Theta_{ws})^2 \times EC_w \times EC_s}{(\Theta_s \times EC_w) + (\Theta_{ws} \times EC_s)}\right] + (\Theta_w - \Theta_{ws}) \times EC_w \quad [6]$$

where the parameters Θ_{ss} and EC_{ss} are abbreviated as Θ_s and EC_s, respectively. This is the nonlinear form of the DPPC equation commonly presented in many of the technical salinity articles by Rhoades (1992, 1996b).

The original purpose of Eq. [6] was to provide a practical means of estimating soil salinity levels, given measurements of both EC_a data and secondary soil properties that influence EC_a (i.e., soil properties other than salinity). According to Eq. [6], the five parameters that combine together to determine EC_a are Θ_w, Θ_s, Θ_{ws}, EC_s, and EC_w. According to Rhoades et al. (1989), these five theoretical parameters could be suitably related to the following four measurable soil properties: EC_e (soil salinity), SP, gravimetric soil water content (Θ_g), and ρ_b, using the following assumed relationships and/or empirical, approximating equations:

Assumed relationships:

$$\Theta_w = \Theta_g \times (\rho_b/100) \quad [7a]$$

$$EC_w = (EC_e \times \rho_b \times SP)/(100 \times \Theta_w) = EC_e \times (SP/\Theta_g) \quad [7b]$$

$$\Theta_s = \rho_b/2.65 \quad [7c]$$

Empirical, approximating equations:

$$\Theta_{ws} = 0.639 \times \Theta_w + 0.011 \quad [7d]$$

$$EC_s = 0.019 \times SP - 0.434 \quad [7e]$$

for $\Theta_w > 0.0305$ and $SP > 25$. (In practical applications, when $\Theta_w < 0.0305$ and/or $SP < 25$, then Θ_{ws} is defined to be equal to Θ_w and/or EC_s is set equal to 0.041, respectively.) Rhoades et al. (1989) also suggested that the ρ_b could be reasonably estimated from the SP in most field survey conditions using the following linear relationship:

$$\rho_b = 1.73 - 0.0067 \times SP \quad [8]$$

Hence, in a practical survey application, Eq. [6] can be solved provided one obtains either accurate field estimates or, preferably, laboratory measurements of EC_e, SP, and Θ_g. For the remainder of this paper, we will refer to such a solution as the calculated EC_a ($CalcEC_a$).

It should be noted that Eq. [6] is designed to produce an estimate of the $CalcEC_a$ referenced to 25°C for the specific depth zone that the soil properties are sampled from. This estimate should correspond on a one-to-one basis to a direct EC_a measurement acquired from the same depth zone (after applying an appropriate temperature compensation). For example, there should be a one-to-one correspondence between this estimate and a conductivity measurement acquired using an insertion four-electrode probe (Rhoades et al., 1989). However, this estimate will not generally exhibit a one-to-one correspondence with an indirect measurement of EC_a, such as conductivity signal data acquired using a noninvasive electromagnetic induction (EM) meter (like the Geonics EM-38 m).[1] There are numerous reasons for this: (i) EM signal data meters obtain a nonlinear, depth-weighted EC_a signal response that is not isolated to a particular depth zone; (ii) the Geonics meter in particular begins to exhibit a partial breakdown in the low induction number approximation (between apparent and true conductivity) when the true terrain conductivity exceeds 100 mS/m; and (iii) variations in the macro surface geometry of the soil environment (such as those induced by a typical bed-furrow structure) tend to exhibit a pronounced effect on the magnitude of the near surface–weighted EC_a signal readings (McNeill, 1980; Lesch et al., 1995a; Rhoades et al., 1999b). (The measurement scales are also different: The EM-38 signal is expressed in mS/m, and the $CalcEC_a$ is typically expressed in dS/m.) Nonetheless, the correlation between the $CalcEC_a$ and measured EM signal response should be quite high, provided a large enough depth zone is sampled (≥ about 1 m) and the position of the instrument relative to the bed-furrow environment is kept constant throughout the survey process (Lesch et al., 1995a).

Definition and Application of a DPPC Correlation Analysis

The original DPPC equation was designed to be used as an EC_e prediction model, given measurements of EC_a

[1] Mention of trademark or proprietary products in this manuscript does not constitute a guarantee or warranty of the property by the USDA and does not imply its approval to the exclusion of other products that may also be suitable.

and either measurements or estimates of the remaining primary soil properties (SP, Θ_w, and ρ_b). However, this equation can also be used in a different, yet equally important manner. Assuming that the underlying model is valid, Eq. [6] can be used in a general-purpose validation procedure for survey data, as described below.

Consider a typical field-scale salinity survey conducted using some type of soil conductivity instrument (such as a Geonics EM-38 meter). Suppose that this process is performed similar to the methodology described in Lesch et al. (1995a, 1995b); i.e., a large number of EM survey sites are acquired across the field, and then a few select sites are identified for calibration soil sampling. Additionally, assume that the soil sample data from these calibration sites are then analyzed for EC_e, SP, and Θ_g. Based on this sample data, what can we infer about the expected correlation between these measured soil properties and the EM-38 signal data?

Obviously, the correlation between the EM signal data and any measured soil property can be directly calculated. However, as alluded to in the introduction, these correlation estimates can change quite radically from one field to the next and therefore often appear inconsistent and/or inconclusive. Clearly, a more desirable approach would be to examine the soil property data directly and then try to derive a general relationship relating these data observations to the acquired signal data.

In essence, this is exactly what the DPPC equation is designed to do. It takes as input a set of primary (i.e., defining) soil properties and produces as output a calculated conductivity ($CalcEC_a$). If this equation can be used produce an accurate estimate of the true (unknown) EC_a, then it should also be highly correlated with the measured EC_a (i.e., the EM sensor readings, acquired at the same calibration locations). Therefore, if this is indeed the case, then the expected correlation between the EM data and any particular primary soil property should be quite similar to the observed correlation between the $CalcEC_a$ and that same soil property.

This correlation concept is shown graphically by the path diagram displayed in Fig. 2. In this diagram, EC_a,[d] represents the true EC_a of the soil within a specific depth

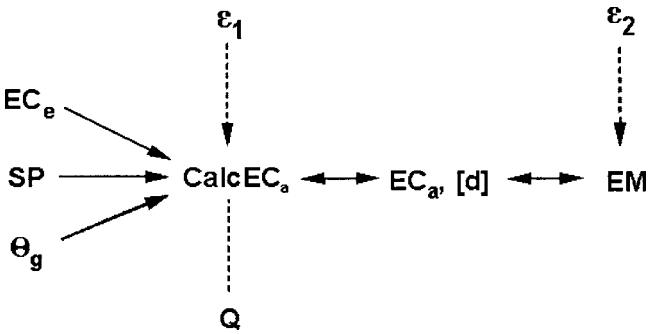

Fig. 2. Path diagram showing the correlation relationships between measured primary [electrical conductivity of the saturated soil extract (EC_e), saturation percentage (SP), and gravimetric soil water content (Θ_g)] and secondary (Q) soil properties, calculated soil electrical conductivity ($CalcEC_a$), measured electromagnetic induction survey data, and true soil electrical conductivity (EC_a,[d]) for depth zone [d].

zone [d]. There are two ways to ascertain this value: (i) measure it directly or indirectly using some type of survey instrument (EM) or (ii) calculate it from the associated primary soil property measurements using an appropriate model ($CalcEC_a$). Both of these approaches are subject to some degree of error (ε_1 and ε_2). For example, errors can occur with respect to the survey data due to instrument miscalibration, signal attenuation, or signal penetration below the depth zone [d] of interest. Likewise, errors may enter into the modeling process due to unrealistic or improper modeling assumptions or less-than-adequate modeling approximations, etc. However, in an ideal situation, we expect these errors to be small and hence the EM and $CalcEC_a$ data to be highly correlated. Mathematically, this can be written as:

$$\text{Corr}(\text{EM}, \text{CalcEC}_a) = \pi \text{ where the limit}(\pi) \rightarrow 1$$
$$\text{as } \varepsilon_1, \varepsilon_2 \rightarrow 0$$

In turn, the $CalcEC_a$ data will exhibit some specific degree of correlation with each of the defining primary soil properties that determine it. These correlation values can be expressed as:

$$\text{Corr}(\text{CalcEC}_a, \text{EC}_e) = \eta 1$$
$$\text{Corr}(\text{CalcEC}_a, \text{SP}) = \eta 2$$
$$\text{Corr}(\text{CalcEC}_a, \Theta_g) = \eta 3$$

Additionally, this $CalcEC_a$ may well correlate with some other soil property (Q) that does not directly determine it. This can occur if the secondary soil property happens to correlate with one or more of the primary soil properties; thus, an induced correlation is said to be present. This secondary correlation can be expressed as:

$$\text{Corr}(\text{CalcEC}_a, Q) = \varsigma 1$$

However, given these correlation estimates, the expected values of the correlation estimates between the EM signal data and each soil property can be shown to be

$$\text{E}[\text{Corr}(\text{EM}, \text{EC}_e)] = \pi \times \eta 1 \quad [9a]$$
$$\text{E}[\text{Corr}(\text{EM}, \text{SP})] = \pi \times \eta 2 \quad [9b]$$
$$\text{E}[\text{Corr}(\text{EM}, \Theta_g)] = \pi \times \eta 3 \quad [9c]$$
$$\text{E}[\text{Corr}(\text{EM}, Q)] = \pi \times \varsigma 1 \quad [9d]$$

(a proof of this result is given in Appendix A.1). In other words, the expected correlation between the EM signal data and a specific soil property is simply the product of the $CalcEC_a$–soil variable correlation multiplied by the EM–$CalcEC_a$ correlation.

Two important conclusions can be immediately deduced from the above results. First, the partitioning of the correlation structure lends itself naturally to an ideal data validation strategy, herein referred to as a *DPPC correlation analysis*. In a DPPC correlation analysis, each of the correlation estimates described above are calculated, in addition to each observed EM–soil property correlation estimate. If an accurate EC_a model is employed and the errors associated with the EM signal data are minimal, then two results should occur. First,

π should be reasonably close to 1. Second, each *observed* EM–soil property correlation estimate should be reasonably close to its expected estimate (as defined above). When these two results do indeed occur, the overall survey process is said to exhibit a *high degree of internal data validity and consistency*.

Second, as the correlation between $CalcEC_a$ and EM approaches unity, the expected EM–soil property correlation estimates reduce to the observed $CalcEC_a$–soil property correlation estimates. This implies that when an accurate soil conductivity model is used, the expected EM–soil property correlation estimates can be approximated by multiplying the observed CalcECa–soil property estimates by some reasonable π value (i.e., 0.9, 0.95, etc.). This is an important point; i.e., this methodology can be used to estimate an expected correlation between EM and soil property in any given field (provided some soil sample data has been collected) *before* an EM survey is undertaken.

Modification of the DPPC Equation for Low Water Content Situations

Water contents substantially in excess of field capacity are not typically of concern in most practical field survey applications because EM or four-electrode surveys are not easily conducted across wet fields. However, survey data sometimes do get collected across fields with water contents significantly below field capacity. In practice, this can occur due to unavoidable timing or scheduling conflicts and/or misinformation about recent irrigation events. Additionally, unforeseen excessive variation in field water content levels can be encountered in some fields due to poor irrigation uniformity.

In general, we have found the DPPC correlation analysis procedure just described to provide a reliable data validation methodology in most salinity survey studies. However, we have also found that this methodology can perform poorly under unusually dry survey conditions. We believe that this poor performance normally occurs due to the attenuating effect (i.e., the drop-off) in EC_a induced by the depletion of the water within the series-coupled soil water pathway. Hence, a need to extend the previously derived DPPC model to handle low water content situations clearly exists. Furthermore, a more robust model should prove useful for determining the specific degree of water content influence on conductivity signal data collected under low water content situations.

The ordinary DPPC model can be made more robust for low water content situations by redefining the Θ_{ws}, Θ_{wc}, and Θ_w water content–partitioning relationship as follows:

$$\Theta_w = \Omega_{ws} + \Omega_{wc} \quad [10]$$

where

$$\Omega_{wc} = \delta \times \Theta_{wc} \quad [11]$$

$$\Omega_{ws} = \Theta_w - \delta \times \Theta_{wc} \quad [12]$$

and Ω_{ws} and Ω_{wc} are the adjusted volumetric soil water contents of series-coupled pathway and continuous liquid pathway, respectively, and δ is defined to be a function of the apparent water content. We have found that good results are obtained if δ is referenced to the water content relative to an estimate of the approximate field capacity (Rhoades et al., 1989). More specifically, assuming that the water content at field capacity (Θ_{fc}) can be approximated as:

$$\Theta_{fc} = (SP \times \rho_b)/200 \quad [13]$$

then the scaled water content relative to field capacity (Δ_w) can be defined as:

$$\Delta_w = \Theta_w/\Theta_{fc} = 2(\Theta_g/SP) \quad [14]$$

In turn, δ can be defined to be a suitable function of Δ_w. One simple, appealing equation that can be used to define δ is the logistic function:

$$G(\delta) = \ln[\delta/(1 - \delta)] = \beta_0 + \beta_1(\Delta_w) \quad [15]$$

where β_0 and β_1 represent hyperparameters that control the shape of the logistic curve. Note that the use of this function restricts δ to lie in the (0,1) interval, with the hyperparameters essentially controlling the degree of apparent water content partitioning.

Based on the approach described above, a new version of the DPPC model can be derived (by replacing Θ_{ws} and Θ_{wc} with Ω_{ws} and Ω_{wc} in Eq. [6]), herein referred to as a dynamic water content partitioning model (Dy-DPPC). This Dy-DPPC model can be expressed as:

$$EC_a = \left[\frac{(\Theta_s + \Omega_{ws})^2 \times EC_w \times EC_s}{(\Theta_s \times EC_w) + (\Omega_{ws} \times EC_s)}\right] + \Omega_{wc} \times EC_w \quad [16a]$$

or equivalently as

$$EC_a = \left[\frac{(\Theta_s + \Theta_w - \delta \times \Theta_{wc})^2 \times EC_w \times EC_s}{(\Theta_s \times EC_w) + [(\Theta_w - \delta \times \Theta_{wc}) \times EC_s]}\right] + \delta \times \Theta_{wc} \times EC_w \quad [16b]$$

where the Ω_{ws} and Ω_{wc} parameters have been replaced with the relationships shown in Eq. [11] and [12]. The effect of incorporating this δ parameter into the ordinary DPPC model is made clear by Eq. [16b]. First, as $\delta \rightarrow 0$, the slope term of Dy-DPPC model reduces to 0 (implying that the apparent conductivity signal strength will be significantly reduced as the soil dries out). Second, as $\delta \rightarrow 1$, this Dy-DPPC model reduces exactly to the ordinary DPPC model (implying that δ can be conditioned to have no effect when the soil is at or near field capacity).

As defined above, the Dy-DPPC model depends critically on the value of δ, which from Eq. [15], is defined to be:

$$\delta = \frac{\exp[\beta_0 + \beta_1(\Delta_w)]}{1 + \exp[\beta_0 + \beta_1(\Delta_w)]} \quad [17]$$

where β_0 and β_1 represent empirical fitting parameters. Figure 3 displays two hypothetical δ curves, and each curve is designed to produce a value of $\delta = 0.5$ when the scaled water content also equals 0.5 ($\Delta_w = 0.5$). The different shapes of these curves are controlled by the magnitude of the β_1 parameter, as indicated in Fig. 3.

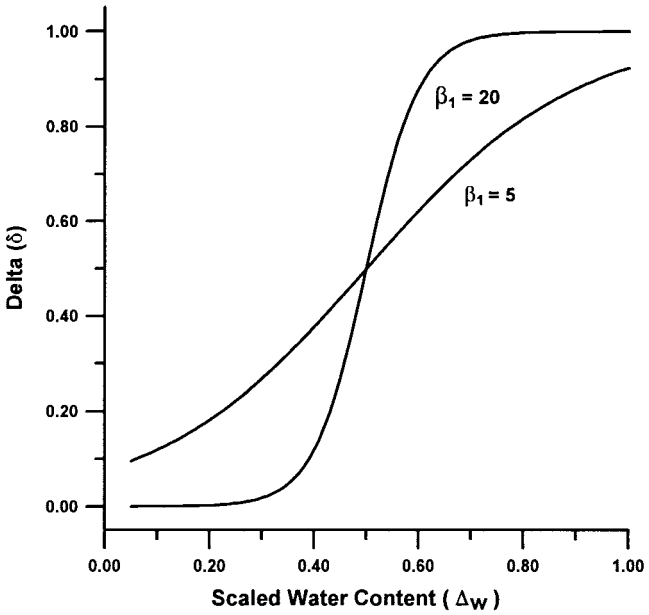

Fig. 3. Two hypothetical dynamic water content–repartitioning parameter (δ) curves which could be used to re-partition the relative volumetric soil water content volumes of series-coupled pathway (Θ_{ws}) and continuous liquid pathway (Θ_{wc}) content in the dynamic water content–partitioning DPPC model (Dy-DPPC). Δ_w, scaled water content relative to field capacity.

The 0.5 curve midpoint values are produced by the β_0 parameter, specifically by setting $\beta_0 = -0.5\beta_1$. Figure 4 shows the corresponding water content repartitioning effects on the Ω_{ws}/Θ_w and Ω_{wc}/Θ_w ratios induced by these assumed δ functions and contrasts these with Θ_{ws}/Θ_w and Θ_{wc}/Θ_w ratios assumed in the ordinary DPPC model.

It is impossible to determine in advance the exact values of β_0 and β_1 in any particular survey situation. However, reasonable bounds can be placed on these parameters, and then the acquired survey and soil sample data can be used to estimate these values via a suitable optimization approach. The approach used here is simply a detailed grid search over the assumed parameter space (as described in the Methods section). Such an optimization approach does not produce any standard error estimates for β_0 and β_1. However, when the correlation is found to increase (over the correlation estimate produced using the ordinary DPPC model calculations), an approximate *F* test can still be constructed to determine if the increase in the correlation estimate is statistically significant (details concerning this test are given in Appendix A.2).

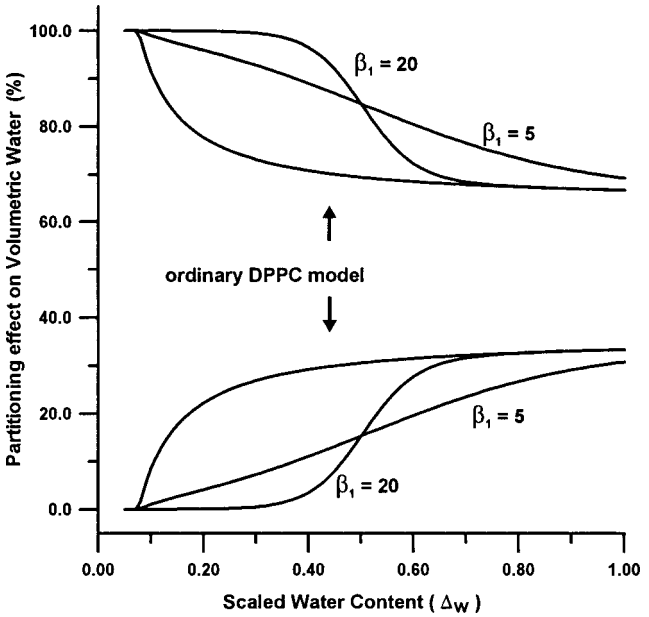

Fig. 4. The degree of (top) Ω_{ws}/Θ_w and (bottom) Ω_{wc}/Θ_w relative percentage water content partitioning induced by the two δ curves shown in Fig. 3, in contrast to the assumed Θ_{ws}/Θ_w and Θ_{wc}/Θ_w curves used in the ordinary DPPC model.

METHODS

Field Survey Information

Survey data from 12 fields are discussed in this paper. These 12 fields have been chosen from a larger database (of 100+ fields) compiled by the Salinity Laboratory over the last decade and represent the range of conditions typically encountered when performing soil salinity surveys.

Table 1 lists the field ID codes, survey area size, and basic soil taxonomy of each survey area. Table 2 lists the types of conductivity and soil variable information collected across these 12 fields. Only Geonics EM-38 conductivity signal data is analyzed although the analysis methods presented here are applicable to any EM and/or insertion four-electrode EC_a signal data. The primary soil properties considered are salinity (EC_e, dS/m); SP (%); the estimated Θ_w (ratio: estimated from the SP and Θ_g); and in one field, the ρ_b (g/cm^3). Some secondary soil properties were also measured in a few of the fields; these secondary properties include the sodium adsorption ratio, B (g/L), and percentage clay (%).

Basic EM-38 and soil sample summary statistics are given in Tables 3a and 3b for each field. These statistics include the

Table 1. Basic soil taxonomy associated with the 12 field survey projects.

Field ID code	Field size	Soil classification
	ha	
CV-W96	16	Gilman fine sandy loam, wet; Gilman silt loam, wet; Indio very fine sandy loam, wet: (Typic Torrifluvents)
CV-K93	16	Salton silty clay loam: (Aquic Torriorthents); Indio very fine sandy loam, wet: (Typic Torrifluvents)
BWD-623	130	Panoche silty clay: (thermic Xerorthents)
CV-T2	14	Salton silty clay loam: (Aquic Torriorthents); Indio very fine sandy loam, wet: (Typic Torrifluvents)
BWD-T1	65	Panoche silty clay: (thermic Xerorthents)
WL-99	32	Lethent clay loam: (Typic Natrargid)
IID-113	16	Imperial-Glenbar silty clay loams, wet: (Vertic Torrifluvents); Meloland very fine sandy loam, wet: (Typic Torrifluvents)
ACA-7	454	Nine mile series: (Entic Haplustols); Whitney soil series (Typic Haplustolls)
IID-34	28	Holtville silty clay, wet: (Typic Torrifluvents)
PV-01	24	Holtville silty clay; Ripley silty clay loam; Gilman silty clay loam: (Typic Torrifluvents)
IID-14	47	Meloland very fine sandy loam, wet; Meloland and Holtvile loams, wet; Vint loamy very fine sand, wet: (Typic Torrifluvents)
CO-4	38	Limon silty clay, fine: (Ustertic Torriorthents); Apishapa silty clay, fine: (Vertic Haplaquepts)

Table 2. Type of survey and soil sample data acquired for the 12 field survey projects.

Variable	Abbreviation	Units
	Conductivity data	
EM-38 signal data	EM_v, EM_h	mS/m
	Primary soil variables	
Salinity	EC_e	dS/m
Saturation percentage	SP	%
Gravimetric water content	Θ_g	%
Volumetric water content	Θ_w	ratio, estimated in all cases except BWD-T1
Bulk density	ρ_b	g/cm^3 (collected at BWD-T1)
	Secondary soil variables	
Sodium adsorption ratio	SAR	ratio (collected at CV-T2, WL-99, CO-4)
Boron	B	mg/L (collected at WL-99)
Percentage clay	% clay	% (collected at BWD-T1)

calculated mean, standard deviation, minimum and maximum reading for each measured variable, along with the number of samples acquired. The number of EM-38 readings in all but one case ranges from 100 to >4000 while the number of soil sample sites ranges from 12 to 40. This oversampling of EM signal data is typical of soil salinity surveys; the goal is to use the abundant, rapidly acquired EM data to infer information about the much more difficult to acquire (i.e., expensive and time consuming to sample) soil data. In most cases, the sampling strategies for the selection of soil sampling sites were developed from model-based site selection techniques similar (or identical) to those described in Lesch et al. (1995b). Additionally, in all but one case, soil samples were collected to a depth of 1.2 m at 0.3-m increments. For the sake of brevity, only the 0- to 1.2-m bulk average data have been analyzed (as reported in Tables 3a and 3b).

Table 3c shows how the 12 fields were divided into two separate groups (A and B), based on each field's calculated soil water content relative to field capacity ($100 \times \Delta_w$). The six Group A fields shown in Table 3a represent surveys where the relative water content data appears to be at or near field capacity. In contrast, the six Group B fields all exhibited relative water content levels significantly below the calculated field capacity. We will show (in the Results section) that the soil water content relative to field capacity represents a critically important parameter when performing a DPPC correlation analysis.

Some additional details concerning each field survey project are given in Table 4. As indicated, 10 of the survey projects were performed within California, but fields CO-4 and ACA-7 were located in Colorado and in Alberta, Canada, respectively. Unless indicated otherwise, EM-38 and soil sample data were collected by George E. Brown, Jr., Salinity Laboratory staff.

Table 3a. Basic field EM-38 and soil sample summary statistics: Group A surveys.

Field ID code	Variable†	*N*	Mean	Standard deviation	Min.	Max.
CV-W96	EM_v	121	40.17	16.74	14.0	109.0
	EM_h	121	24.12	13.58	5.0	74.0
	EC_e	16	2.326	1.423	0.845	6.641
	SP	16	40.39	2.86	36.47	45.79
	Θ_w	16	0.236	0.042	0.178	0.322
CV-K93	EM_v	139	141.99	41.41	64.0	260.0
	EM_h	139	95.37	33.50	36.0	196.0
	EC_e	16	10.046	3.347	5.365	16.80
	SP	16	56.95	2.96	51.01	61.05
	Θ_w	16	0.378	0.018	0.334	0.408
BWD-623	EM_v	128	121.39	31.53	57.0	188.0
	EM_h	128	83.10	22.37	33.0	134.0
	EC_e	16	3.653	1.656	1.608	8.194
	SP	16	50.30	14.07	33.18	85.01
	Θ_w	16	0.308	0.054	0.214	0.392
CV-T2	EM_v	100	172.36	52.07	76.0	344.0
	EM_h	100	130.80	49.43	52.0	276.0
	EC_e	15	11.776	6.020	3.725	22.89
	SP	15	63.32	2.13	59.68	66.73
	Θ_w	15	0.325	0.018	0.301	0.361
	SAR	15	23.23	12.33	5.548	40.19
	B	15	1.435	0.649	0.520	2.569
BWD-T1	EM_v	100	133.64	19.10	88.0	192.0
	EM_h	100	85.20	12.62	56.0	124.0
	EC_e	16	2.666	1.400	0.900	5.688
	SP	16	55.42	7.30	40.59	67.35
	Θ_w	16	0.380	0.034	0.291	0.420
	ρ_B	16	1.346	0.057	1.256	1.438
	% clay	16	35.27	6.02	23.77	44.49
WL-99	EM_v	384	488.22	99.83	256.4	795.3
	EM_h	384	292.80	70.61	144.6	519.4
	EC_e	40	20.191	5.030	12.83	36.60
	SP	40	59.79	7.81	45.83	78.94
	Θ_w	40	0.342	0.036	0.274	0.415
	SAR	40	50.90	13.06	30.00	88.78
	B	40	17.81	4.01	11.67	29.08

† See Table 2 for variable defiinitions and units.

Table 3b. Basic field EM-38 and soil sample summary statistics: Group B surveys.

Field ID code	Variable†	*N*	Mean	Standard deviation	Min.	Max.
IID-113	EM_v	1929	89.13	17.53	46.0	142.0
	EM_h	1929	89.57	15.49	51.0	123.0
	EC_e	12	4.800	1.743	2.698	8.395
	SP	12	52.08	4.35	44.90	59.23
	Θ_w	12	0.203	0.044	0.131	0.279
ACA-7	EM_v	35	68.46	63.08	10.0	314.0
	EC_e	35	3.298	4.140	0.430	20.51
	SP	35	52.61	11.77	36.50	83.50
	Θ_w	35	0.192	0.047	0.080	0.265
IID-34	EM_v	4043	93.98	15.53	45.0	139.0
	EM_h	4043	83.97	13.73	43.0	122.0
	EC_e	12	2.916	0.778	1.858	4.815
	SP	12	57.22	6.39	46.05	65.98
	Θ_w	12	0.238	0.051	0.145	0.308
PV-01	EM_v	1766	103.58	40.41	30.0	304.0
	EM_h	1766	75.72	28.60	17.0	207.0
	EC_e	12	3.038	2.491	1.187	10.46
	SP	12	67.80	17.16	43.77	92.17
	Θ_w	12	0.276	0.050	0.181	0.326
IID-14	EM_v	4474	100.16	19.91	45.0	165.0
	EM_h	4474	68.24	13.51	29.0	109.0
	EC_e	12	3.701	2.437	1.512	10.38
	SP	12	48.98	9.91	32.80	60.70
	Θ_w	12	0.216	0.063	0.100	0.272
CO-4	EM_v	93	147.18	83.93	20.0	328.0
	EM_h	93	107.14	62.77	12.0	264.0
	EC_e	15	10.423	4.323	3.873	17.19
	SP	15	63.41	17.75	35.23	90.54
	Θ_w	15	0.229	0.046	0.148	0.300
	SAR	15	20.31	8.63	8.26	34.89

† See Table 2 for variable definitions and units.

Table 3c. Scaled water content summary statistics (% basis): Groups A and B (note: percentage water | field capacity calculated as 100 × Δ_w, where Δ_w = scaled water content relative to field capacity).

Field ID code	Mean	Standard deviation	Min.	Max.
		Group A surveys		
CV-W96	79.85	9.87	65.25	102.49
CV-K93	98.65	7.23	85.56	111.34
BWD-623	90.35	7.52	69.29	101.18
CV-T2	78.68	4.67	70.98	86.10
BWD-T1	103.62	4.34	98.55	111.00
WL-99	87.69	8.53	68.88	103.50
		Group B surveys		
IID-113	56.25	10.58	37.12	71.87
ACA-7	56.18	15.66	23.80	87.26
IID-34	61.44	9.95	44.55	77.93
PV-01	66.51	5.67	56.88	74.48
IID-14	63.30	13.96	36.23	81.27
CO-4	58.72	13.24	37.52	82.93

Additionally, in all but one case, the EM-38 signal data consists of both horizontal and vertical readings, and soil variable information (as reported in Tables 3a, 3b, and 3c) represents the arithmetic average of four 30-cm samples acquired from a 0- to 1.2-m sampling depth.

Data Analysis

In 11 of the 12 survey projects, both horizontal and vertical conductivity readings were acquired at each sample site. Hence, these readings had to first be combined into a single, average EM value before the $CalcEC_a$–conductivity correlation estimate could be computed. Additionally, because both the EM signal conductivity readings and soil chemical data exhibited highly right-skewed (i.e., lognormal) data distributions, all of these data were log-transformed before the correlation analyses were performed. (This log transformation helped stabilize the correlation estimates and correct for the nonlinear EM signal response in fields with readings above 100 mS/m.)

The 12 ordinary DPPC correlation analyses were calculated as follows. First, in all fields except BWD-T1, the ρ_b was estimated using Eq. [8]. Next, the $CalcEC_a$ data vector was computed using the ordinary DPPC model (Eq. [6]), after calculating the values of the appropriate model parameters using Eq. [7a] through [7e]. The EM signal data, computed $CalcEC_a$ data, and all soil chemical data were then log-transformed, and the average EM signal level was defined to be $\ln(EM_{avg}) = 0.5[\ln(EM_v) + \ln(EM_h)]$, where EM_v and EM_h are EM-38 vertical and horizontal signal data, respectively. All of the relevant, individual DPPC correlation estimates were then calculated. Finally, the predicted EM–soil variable correlation estimates were computed using the correlation product relationship (Eq. [9a] through [9d]), and approximate 95% confidence intervals for each of these predictions were constructed (using the 95% confidence interval formula described in Appendix A.3).

As explained previously, the Dy-DPPC model (Eq. [16b]) depends on both the ordinary (prespecified) DPPC model parameters and an additional δ parameter, which itself is modeled as a function of the observed scaled water content. The assumed g(δ) logistic function (Eq. [17]) describes this relationship and in turn depends on two new, unknown parameters (β_0 and β_1).

Optimized estimates for β_0 and β_1 were obtained for the Dy-DPPC model by maximizing the observed $\ln(CalcEC_a)$–$\ln(EM_{avg})$ correlation estimate over a prespecified (β_0, β_1) parameter space. This was performed directly, i.e., by employing a detailed grid search over a range of suitable β_0 and β_1 values and then choosing the pair of (b_0, b_1) values that produced the maximum correlation estimate. Bounds for the search grid were specified by constraining the curve midpoint value to lie within an interval of 0.25 to 0.75 and restricting the slope parameter to lie within the interval of 2 to 25 [implying that $\beta_1 \in (2,25)$ and $\beta_0 \in (-0.75\beta_1, -0.25\beta_1)$]. The first range reflected the assumption that δ might potentially assume a value of 0.5 anywhere within a water content range of 25 to 75% field capacity. In a similar manner, the β_1 range endpoints were selected to reflect a potentially wide adjustment in the slope of the δ curve.

When optimized (b_0, b_1) values were determined, the statistical significance of the improved $\ln(CalcEC_a)$–$\ln(EM_{avg})$ correlation estimate was judged using the *F* score test results. In these analyses, a significance level of $\alpha = 0.1$ was used to indicate significant vs. nonsignificant improvement. If the improvement in the primary correlation estimate was found to be statistically significant, a new DPPC correlation analysis was performed using the optimized Dy-DPPC model in place of the ordinary DPPC model.

All of the statistical quantities pertaining to the above analyses (DPPC correlation estimates, *F* tests, and 95% correlation confidence intervals) were calculated using the ESAP-Calibrate software program, Version 2.21, and verified using SAS Version 8.1 (SAS Inst., 1999).

RESULTS

Ordinary DPPC Correlation Analysis Results

Table 5a lists the DPPC results from the six Group A correlation analyses, corresponding to the six fields

Table 4. Additional survey details concerning all 12 field survey projects.

Field ID code	General location	Sampling date	Crop type†	Survey type	Data source‡	Notes§
CV-W96	Coachella, CA	1996	Wheat	Grid survey	a	
CV-K93	Coachella, CA	1993	Fallow	Grid survey	a	
BWD-623	Broadview, CA	1991	Cotton	Grid survey	a, b	
CV-T2	Coachella, CA	1997	Sorghum	Grid survey	a, c(2)	
BWD-T1	Broadview, CA	1996	Cotton	Grid survey	a, c(1)	
WL-99	Westlands, CA	1999	Fallow	Grid survey	d	
IID-113	Imperial, CA	2000	Alfalfa	Transect survey	e	
ACA-7	Pine Coulee, AB, Canada	1998	Oat	Point samples	f	1
PV-01	Palo Verde, CA	2001	Fallow	Transect survey	g	2
IID-14	Imperial, CA	2001	Alfalfa	Transect survey	e	
CO-4	Pleblo, CO	1995	Alfalfa	Grid survey	h	

† Wheat, *Triticum aestivum* L.; cotton, *Gossypium hirsutum* L.; sorghum, *Sorghum bicolor* (L.) Moench; alfalfa, *Medicago sativa* L.; oat, *Avena sativa* L.

‡ a, Corwin and Lesch (2003); b, Corwin et al. (1999); c, Lesch et al. (2000): 1 = ESAP Version 2.01 training file no. 1 and 2 = ESAP Version 2.01 training file no. 2; d, Corwin et al. (2003); e, data collected by Imperial Irrigation district salinity assessment program (used with permission); f, data collected by Genesis Environmental (used with permission); g, data collected by Soil and Water West (used with permission); h, archived GEBJ Salinity Laboratory survey data (not previously published).

§ 1 = EM, data only, collected only at soil sampling locations, and sites subjectively selected off visual height and vigor of hay crop; 2 = soil samples in this field collected in 30-cm increments down to a depth of 0.9 m only.

Table 5a. Dual-pathway parallel conductance (DPPC) correlation analysis results: Group A surveys using ordinary DPPC model.

Field ID code	π†	*i*th soil variable‡	$\eta(i)$§	$\pi \times \eta(i)$¶	95% CI#	$\lambda(i)$††
CV-W96	0.895	ln(EC_e)	0.966	0.865	[0.806, 0.924]	0.873
		SP	0.843	0.754	[0.631, 0.878]	0.776
		Θ_w	0.814	0.729	[0.596, 0.862]	0.760
CV-K93	0.855	ln(EC_e)	0.983	0.841	[0.792, 0.890]	0.891
		SP	0.074	0.064	[−0.202, 0.329]	−0.200
		θ_w	0.224	0.191	[−0.068, 0.451]	0.265
BWD-623	0.956	ln(EC_e)	0.713	0.682	[0.576, 0.787]	0.620
		SP	0.821	0.785	[0.700, 0.871]	0.835
		Θ_w	0.840	0.804	[0.722, 0.885]	0.864
CV-T2	0.944	ln(EC_e)	0.995	0.940	[0.923, 0.957]	0.943
		SP	−0.324	−0.306	[−0.471, −0.140]	−0.326
		Θ_w	0.762	0.720	[0.607, 0.833]	0.767
		ln(SAR)	0.937	0.885	[0.824, 0.946]	0.891
		ln(B)	0.921	0.870	[0.802, 0.938]	0.909
BWD-T1	0.949	ln(EC_e)	0.855	0.812	[0.728, 0.896]	0.801
		SP	0.569	0.540	[0.407, 0.673]	0.498
		Θ_w	0.613	0.582	[0.454, 0.710]	0.595
		ρB	−0.402	−0.382	[−0.530, −0.233]	−0.352
		% clay	0.371	0.352	[0.202, 0.502]	0.293
WL-99	0.819	ln(EC_e)	0.889	0.728	[0.644, 0.811]	0.815
		SP	0.514	0.421	[0.265, 0.576]	0.223
		Θ_w	0.514	0.421	[0.265, 0.576]	0.534
		ln(SAR)	0.895	0.733	[0.652, 0.814]	0.745
		ln(B)	0.318	0.260	[0.088, 0.433]	0.404

† π = Corr[ln(EM_{avg}), ln($CalcEC_a$)], where EM_{avg} is average electromagnetic induction and $CalcEC_a$ is calculated soil electrical conductivity.
‡ See Table 2 for variable definitions.
§ $\eta(i)$ = Corr[ln($CalcEC_a$), *i*th soil variable].
¶ $\pi \times \eta(i)$ = predicted Corr[ln(EM_{avg}), *i*th soil variable].
# 95% CI = 95% confidence interval for $\pi \times \eta(i)$.
†† $\lambda(i)$ = Corr[ln(EM_{avg}), *i*th soil variable].

exhibiting high relative water content levels during the actual survey processes. Five of the six ln($CalcEC_a$)–ln(EM_{avg}) correlation estimates exceed 0.85, and three of these values appear to be around 0.95. Additionally, the vast majority of the predicted ln(EM_{avg})–soil property correlation estimates agree well with the observed estimates. The only notable exceptions are associated with the CV-K93 and WL-99 survey data. With respect to the CV-K93 data, the observed ln(EM_{avg})–ln(EC_e) and ln(EM_{avg})–SP estimates of 0.891 and −0.200 appear to fall right on the edge of the corresponding 95% confidence intervals associated with the predicted estimates, which were 0.841 and 0.064, respectively. A similar pattern is evident in the WL-99 data.

Table 5b lists the equivalent DPPC results from the six Group B correlation analyses, corresponding to the six fields exhibiting relative water content levels that are lower than normal. In general, these results do not appear to be as good as the results shown in Table 5a. Two of the six ln($CalcEC_a$)–ln(EM_{avg}) correlation esti-

Table 5b. Dual-pathway parallel conductance (DPPC) correlation analysis results: Group B surveys using ordinary DPPC model.

Field ID code	π†	*i*th soil variable‡	$\eta(i)$§	$\pi \times \eta(i)$¶	95% CI#	$\lambda(i)$††
IID-113	0.480	ln(EC_e)	0.880	0.423	[0.172, 0.673]	0.151
		SP	0.488	0.234	[−0.227, 0.695]	0.472
		Θ_w	0.281	0.135	[−0.372, 0.642]	0.854
ACA-7	0.932	ln(EC_e)	0.973	0.908	[0.879, 0.936]	0.891
		SP	0.721	0.672	[0.587, 0.757]	0.689
		Θ_w	0.223	0.208	[0.089, 0.328]	0.411
IID-34	0.524	ln(EC_e)	0.641	0.336	[−0.058, 0.729]	−0.210
		SP	0.751	0.394	[0.055, 0.732]	0.772
		Θ_w	0.633	0.331	[−0.066, 0.729]	0.905
PV-01	0.901	ln(EC_e)	0.755	0.680	[0.508, 0.851]	0.525
		SP	0.823	0.742	[0.593, 0.890]	0.886
		Θ_w	0.712	0.641	[0.458, 0.825]	0.794
IID-14	0.915	ln(EC_e)	0.746	0.682	[0.520, 0.844]	0.689
		SP	0.628	0.574	[0.385, 0.764]	0.567
		Θ_w	0.834	0.763	[0.629, 0.897]	0.797
CO-4	0.909	ln(EC_e)	0.965	0.877	[0.819, 0.935]	0.912
		SP	0.883	0.802	[0.698, 0.907]	0.755
		Θ_w	0.606	0.550	[0.373, 0.737]	0.728
		ln(SAR)	0.966	0.878	[0.820, 0.935]	0.927

† π = Corr[ln(EM_{avg}), ln($CalcEC_a$)], where EM_{avg} is average electromagnetic induction and $CalcEC_a$ is calculated soil electrical conductivity.
‡ See Table 2 for variable definitions.
§ $\eta(i)$ = Corr[ln($CalcEC_a$), *i*th soil variable].
¶ $\pi \times \eta(i)$ = predicted Corr[ln(EM_{avg}), *i*th soil variable].
# 95% CI = 95% confidence interval for $\pi \times \eta(i)$.
†† $\lambda(i)$ = Corr[ln(EM_{avg}), *i*th soil variable].

Table 6. Ordinary dual-pathway parallel conductance (DPPC) vs. optimized dynamic water content partitioning (Dy-DPPC) modeling results.

Field ID code	Ordinary DPPC π†	Optimized Dy-DPPC π	Model comparison F score ($P > F$)	δ hyperparameters‡	
				$-b_0/b_1$	b_1
CV-W96	0.895	na			
CV-K93	0.855	0.870	1.727 (0.2192)		
BWD-623	0.956	0.962	1.914 (0.1900)		
CV-T2	0.944	0.946	1.229 (0.3299)		
BWD-T1	0.949	0.954	1.718 (0.2208)		
WL-99	0.819	0.871	8.038 (0.0013)	0.63	6.50
IID-113	0.480	0.913	19.16 (0.0009)	0.59	23.25
ACA-7	0.932	0.942	3.543 (0.0411)	0.56	2.75
IID-34	0.524	0.903	15.57 (0.0017)	0.70	20.00
PV-01	0.901	0.933	3.259 (0.0922)	0.74	3.50
IID-14	0.915	0.920	1.288 (0.3273)		
CO-4	0.909	0.941	4.437 (0.0387)	0.42	7.75

† π = Corr[ln(EM_{avg}), ln($CalcEC_a$)], where EM_{avg} is average electromagnetic induction and $CalcEC_a$ is calculated soil electrical conductivity.
‡ $-b_0/b_1$ constrained to lie between [0.25, 0.75]; b_1 constrained to lie between [2.0, 25.0].

mates appear to be extremely poor (fields IID-113 and IID-34, with estimates of 0.480 and 0.524, respectively). These poor primary correlation estimates suggest that the ordinary DPPC model is incapable of reproducing the observed survey–soil property correlation structure in these two fields. Furthermore, many of the predicted ln(EM_{avg})–soil property correlation estimates associated with the remaining four fields appear to be rather different from the observed estimates. Statistically significant differences show up between the predicted vs. observed ln(EM_{avg})–Θ_w estimates in fields ACA-7 and CO-4. Nearly significant differences are apparent in about half of the remaining predicted vs. observed correlation estimates. Overall, the only survey where all of the results seem satisfactory appears to be field IID-14.

Optimized Dy-DPPC Correlation Analysis Results

The preceding results suggest that a DPPC correlation analysis using the ordinary DPPC model generally yields very good results when the water content is near field capacity but can produce less-than-adequate results when applied to survey data collected under low water content conditions. In those instances, the more robust Dy-DPPC model (Eq. [16b]) should be employed.

Table 6 lists the optimized Dy-DPPC modeling results for the 12 case studies previously discussed. One field failed to optimize (CV-W96), but the primary ln($CalcEC_a$)–ln(EM_{avg}) correlation estimates exhibited at least some degree of improvement in the remaining 11 fields. For fields IID-113 and IID-34, the improvement in the ln($CalcEC_a$)–ln(EM_{avg}) correlation was found to be substantial. Overall, the improvement in the primary correlation estimate in six of the fields was judged to be statistically significant, according to the *F*-test results. The final δ hyperparameter estimates for these six fields are also shown in Table 6.

Table 7 lists the new, optimized DPPC correlation results for the six fields where the Dy-DPPC model was

Table 7. Dual-pathway parallel conductance (DPPC) correlation analysis results for surveys WL-99, IID-113, ACA-7, IID-34, PV-01, and CO-4 using the optimized dynamic water content partitioning (Dy-DPPC) model.

Field ID code	π†	*i*th soil variable‡	$\eta(i)$§	$\pi \times \eta(i)$¶	95% CI#	$\lambda(i)$††
WL-99	0.871	ln(EC_e)	0.872	0.760	[0.684, 0.836]	0.815
		SP	0.368	0.321	[0.177, 0.465]	0.223
		Θ_w	0.696	0.606	[0.495, 0.718]	0.534
		ln(SAR)	0.855	0.745	[0.664, 0.825]	0.745
		ln(B)	0.494	0.430	[0.296, 0.565]	0.404
IID-113	0.913	ln(EC_e)	0.203	0.185	[−0.055, 0.425]	0.151
		SP	0.657	0.600	[0.415, 0.785]	0.472
		Θ_w	0.919	0.839	[0.742, 0.936]	0.854
ACA-7	0.942	ln(EC_e)	0.947	0.892	[0.855, 0.929]	0.891
		SP	0.723	0.681	[0.602, 0.760]	0.689
		Θ_w	0.316	0.298	[0.190, 0.406]	0.411
IID-34	0.903	ln(EC_e)	−0.069	−0.063	[−0.321, 0.196]	−0.210
		SP	0.864	0.780	[0.650, 0.910]	0.772
		Θ_w	0.993	0.896	[0.864, 0.927]	0.905
PV-01	0.933	ln(EC_e)	0.570	0.532	[0.353, 0.710]	0.525
		SP	0.922	0.860	[0.776, 0.944]	0.886
		Θ_w	0.859	0.801	[0.690, 0.912]	0.794
CO-4	0.941	ln(EC_e)	0.950	0.895	[0.839, 0.950]	0.912
		SP	0.773	0.727	[0.613, 0.841]	0.755
		Θ_w	0.783	0.737	[0.625, 0.849]	0.728
		ln(SAR)	0.963	0.906	[0.858, 0.955]	0.927

† π = Corr[ln(EM_{avg}), ln($CalcEC_a$)], where EM_{avg} is average electromagnetic induction and $CalcEC_a$ is calculated soil electrical conductivity.
‡ See Table 2 for variable defiintions.
§ $\eta(i)$ = Corr[ln($CalcEC_a$), *i*th soil variable].
¶ $\pi \times \eta(i)$ = predicted Corr[ln(EM_{avg}), *i*th soil variable].
# 95% CI = 95% confidence interval for $\pi \times \eta(i)$.
†† $\lambda(i)$ = Corr[ln(EM_{avg}), *i*th soil variable].

Table 8. Sample data associated with field IID-34. The scaled water content (Δ_w) is used to calculate the dynamic water repartitioning parameter (δ), which in turn is used to transform the ordinary dual-pathway parallel conductance (DPPC) water content parameters (Θ_{wc} and Θ_{ws}) into the dynamic DPPC water content parameters (Ω_{wc} and Ω_{ws}).

Site code	EM_v†	EM_h†	EC_e†	SP†	Θ_w†	Δ_w	δ	Ordinary DPPC model			Dynamic DPPC model		
								Θ_{wc}	Θws	$CalcEC_a$‡	Ω_{wc}	Ω_{ws}	$CalcEC_a$
314	65	58	2.105	46.05	0.1451	0.443	0.006	0.0414	0.1037	0.727	0.0002	0.1448	0.379
268	73	58	3.418	49.00	0.1790	0.521	0.027	0.0536	0.1254	1.102	0.0015	0.1776	0.482
1196	81	73	4.815	53.55	0.1964	0.535	0.036	0.0599	0.1365	1.557	0.0021	0.1943	0.603
2776	95	85	2.993	65.35	0.2300	0.545	0.043	0.0720	0.1579	1.466	0.0031	0.2269	0.851
1961	65	64	3.535	53.08	0.2055	0.564	0.061	0.0632	0.1423	1.271	0.0039	0.2017	0.613
2364	94	85	1.858	51.95	0.2120	0.591	0.101	0.0655	0.1465	0.874	0.0066	0.2054	0.583
3167	106	95	3.108	59.38	0.2485	0.628	0.192	0.0787	0.1698	1.388	0.0151	0.2333	0.874
3716	90	92	2.598	65.98	0.2853	0.671	0.361	0.0920	0.1933	1.458	0.0332	0.2521	1.128
3779	107	107	2.480	62.20	0.2807	0.687	0.436	0.0903	0.1903	1.335	0.0394	0.2413	1.064
2087	105	83	2.443	58.63	0.2708	0.691	0.454	0.0868	0.1840	1.231	0.0394	0.2314	0.978
683	118	105	3.010	60.90	0.2894	0.719	0.593	0.0935	0.1959	1.459	0.0555	0.2339	1.212
3122	127	101	2.633	60.55	0.3081	0.768	0.797	0.1002	0.2078	1.375	0.0799	0.2282	1.272

† See Table 2 for variable definitions.
‡ $CalcEC_a$, calculated soil electrical conductivity.

found to produce a statistically significant improvement in the primary correlation estimate. Five of the six $\ln(CalcEC_a)$–$\ln(EM_{avg})$ correlation estimates now exceed 0.9, and all but one of the predicted $\ln(EM_{avg})$–soil variable correlation estimates now agree well with the observed estimates. These results suggest that the optimized repartitioning of the DPPC water content parameters substantially improves the model's ability to correctly reproduce the observed survey–soil variable data correlation estimates under low water content situations.

An example of the intermediate calculation details associated with both models is shown in Table 8 for field IID-34. This table shows the raw EM-38 and soil sample data for each calibration sample site, along with the intermediate calculations used to estimate both the ordinary DPPC and the Dy-DPPC model. As shown in Table 8, the value of the water content–partitioning parameter (δ) ranged from 0.006 to 0.797. In turn, this has a pronounced effect on the dynamic water content parameter estimates (Ω_{wc} and Ω_{ws}), which are quite different from the ordinary DPPC parameter estimates (Θ_{wc} and Θ_{ws}).

The overall effect of this adjusted water content partitioning is shown in Fig. 5a and 5b. Figure 5a shows the apparent correlation structure between the log-calculated conductivity using the ordinary DPPC model and the average of the log EM signal measurements (r = 0.524). Figure 5b shows the new correlation structure between the log-calculated conductivity using the optimized Dy-DPPC model and the same log EM signal measurements (r = 0.903). This pronounced improvement in the correlation structure suggests that the relatively low water content levels significantly affected (i.e., dampened) the EM signal measurements in this field.

DISCUSSION

Most agricultural EC_a surveys are done with the expressed goal of gaining information about the spatial distribution of one or more soil properties from the acquired conductivity data. Generally, this information is quantified by using some type of statistical modeling procedure (i.e., an empirical equation that can calibrate soil sample data with EC_a signal data). While such an approach has obvious advantages, it lacks an objective technique for judging the validity of the instrument and soil sample data as a whole.

The results from a DPPC correlation analysis can prove to be extremely useful with respect to this issue. First, they provide the analyst with an objective way to judge the general validity of the data set, via the calculation of both the primary CalcECa–EM correlation estimate (this value should be close to 1) and the secondary predicted EM–soil variable correlation estimates (these values should closely match the corre-

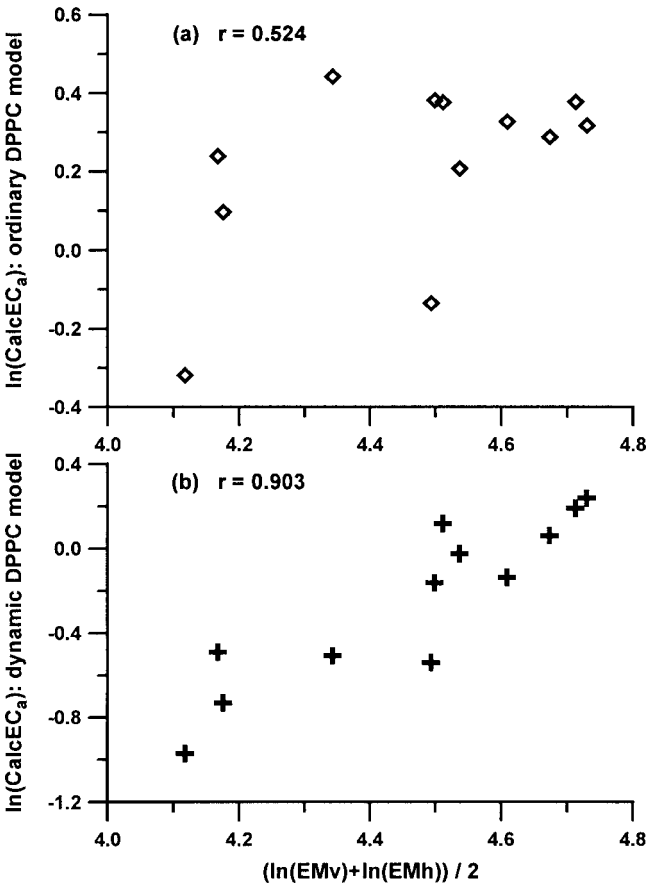

Fig. 5. Calculated soil electrical conductivity ($CalcEC_a$) vs. electromagnetic induction (EM) correlation results in field IID-34 from (a) ordinary DPPC model and (b) optimized, dynamic water content–partitioning DPPC model.

sponding observed estimates). Second, the results from such an analysis represent an excellent procedure for classifying the expected degree of correlation between specific soil properties and the acquired EC_a data. They automatically yield the exact correlation levels between each soil property and the model-calculated conductivity ($CalcEC_a$); multiplying each of these values by the primary $CalcEC_a$–EM correlation level yields the corresponding predicted values. Hence, provided prior soil sample data is available and the employed DPPC model is realistic, this procedure can be used to *project* the expected EM–soil variable correlation levels. This technique is especially useful in precision-farming applications where the target variable of interest is often something other than salinity (Corwin and Lesch, 2003).

Of course, the final accuracy inherent in a DPPC correlation analysis depends on the validity of the model itself. When the relative soil water content level is at or near field capacity, the ordinary DPPC equation generally produces excellent results. In our surveying experiences, fields like WL-99 represent the exception and tend to occur infrequently. However, when the relative water content drops substantially below field capacity, the assumptions inherent in the ordinary equation can begin to break down. More specifically, these analyses suggest that the projected vs. observed correlation results can often be significantly improved by dynamically repartitioning the Θ_{ws} and Θ_{wc} water content components. The method proposed for achieving this (a logistic function conditioned on the scaled water content) does not represent the only conceivable partitioning strategy, but we have found this approach to produce both robust and accurate results in practice.

Based on the limited number of low water content data sets analyzed herein, the δ hyperparameter estimates (β_0 and β_1, shown in Table 6) appear to be quite variable from field to field. This suggests that these parameters are probably field specific and perhaps influenced by other secondary soil physicochemical properties. Additionally, a careful analysis of Eq. [3] shows that the primary DPPC water content parameters (Θ_{ws} and Θ_{wc}) are inherently confounded with the assumption of conductivity equilibrium ($EC_w = EC_{ws} = EC_{wc}$). Hence, the variation in the δ hyperparameter estimates might also reflect field-specific nonequilibrium effects because this latter assumption could also be expected to break down under low water content situations. Nonetheless, the minimum *safe* relative water content level appears to be fairly stable. Specifically, it appears that the repartitioning effect does not generally become a serious issue unless the relative water content drops below 65% (Table 3c). Hence, when conducting a salinity survey, we recommend that the minimum water content with respect to field capacity be kept above 65% whenever possible.

The fact that the ordinary DPPC equation may break down under abnormally low water content situations is actually not surprising. On the contrary, this problem is discussed in detail in Rhoades et al. (1999b), along with a number of important reasons for not performing soil conductivity surveys under low water content situations. Additionally, the use of the modified Dy-DPPC model does not mitigate this concern in any practical sense. In other words, although the Dy-DPPC model was successfully used to verify that the observed high EM–water content and low EM–salinity correlations were correct (in a data validation sense), this does not imply that the low EM–salinity correlation problem can be corrected. To achieve such a correction, one would need fairly precise water content estimates at each and every survey site, e.g., either actual water content measurements across the entire survey grid or a second set of instrument signal data that could be used to accurately estimate the spatial variation in soil water content. Neither type of measurement data is available for any of the 12 survey projects examined here. Hence, even though all 12 survey projects exhibit high internal validity, some of the survey processes will still clearly fail to yield accurate salinity maps (e.g., fields IID-113 and IID-34).

From a more general data interpretation perspective, these DPPC correlation analysis results demonstrate why there is often such significant variation in the various EM signal data–soil variable correlation estimates between different fields. As discussed in Corwin and Lesch (2003), the final correlation estimates in any specific survey situation are strongly influenced by *both* the variability of each (primary) soil property and the degree of correlation between these properties. Additionally, the degree of dynamic water partitioning (under low water content situations) will also have a pronounced effect. For example, when EC_e represents the dominant soil property and the soil is near field capacity, the EC_a–EC_e correlation level is nearly always quite high. High correlation levels between the EC_a and other soil properties (SP, percentage clay, Θ_w, etc.) typically only occur when these other properties simultaneously correlate well with salinity. However, as these other primary soil properties become more variable *and* less correlated with salinity, the EC_a–EC_e correlation level tends to drop off. Additionally, as the spatial variation in soil salinity decreases and the spatial variation in the other primary properties increases, one or more of these other properties will eventually supercede the soil salinity as the dominant soil property. Furthermore, as shown herein, if the relative water content drops too far below field capacity, then the spatial variation in water content can become the dominant factor influencing the EC_a data, even in the presence of large spatial variation in salinity.

In general, the preceding analyses demonstrate the degree of potential variation that often occurs in EC_a–soil property correlation estimates. A multitude of results are possible, but the final correlation levels ultimately depend on the joint distribution and relative spatial variation inherent in the primary soil properties. The simultaneous interaction of all of these properties must first be quantified before an accurate projection of the EC_a–soil property correlation structure can be made. However, given such information, the preceding results suggest that accurate projections are possible under a wide variety of typical surveying conditions.

CONCLUSION

The aforementioned analyses demonstrate the usefulness of the DPPC modeling approach, from both a

specific data validation perspective and a more general data interpretation perspective. These results demonstrate how the DPPC model developed by Rhoades et al. (1989) can be used to accurately predict the expected correlation structure between EC_a data and multiple soil properties of interest for an arbitrary survey process. This methodology (referred to as a DPPC correlation analysis) represents a useful survey data validation procedure as well as a quantitative technique for describing how different soil properties correlate with the acquired EC_a data. These results indicate that this technique generally works well in practice, provided the relative soil water content across the survey area is reasonably close to field capacity.

The ordinary DPPC model can be extended to handle survey data collected under low water content situations through the use of an adjusted, field-specific water content–partitioning function. A simple partitioning strategy has been presented, along with a technique for estimating and testing the partitioning hyperparameters for statistical significance. Results from 12 different salinity surveys suggest that this adjustment can induce a substantial improvement in the accuracy of the predicted correlation structure under especially low water content situations. However, low soil water content situations should still be avoided during actual EM–salinity survey applications because there is no way to adjust for the heightened water content effect at any of the noncalibration survey sites.

In a broader sense, these results demonstrate that the correlation structure between survey conductivity data and different soil properties in any specific field can be quite variable. This structure ultimately depends on the joint distribution of the primary EC_e, SP, and Θ_w soil properties (under normal water content conditions) and also the degree of assumed continuous vs. series-coupled water content partitioning (under low water content conditions).

APPENDIX

Part A.1

A proof of the correlation product relationship can be developed as follows. Let X, Y, and Z represent three stochastic random variables with finite mean and variance, with the variance of Y defined as σ_Y^2. Suppose that both X and Z are related to Y in a linear manner, i.e.,

$$X = A_0 + A_1(Y) + \varepsilon_1, \text{ where } \varepsilon_1 \sim \text{iid } N(0, \eta_1^2)$$
$$Z = B_0 + B_1(Y) + \varepsilon_2, \text{ where } \varepsilon_2 \sim \text{iid } N(0, \eta_2^2)$$

and that the residual error components (ε_1 and ε_2) are independent. Then, if $\text{Corr}(X,Y) = \rho_{XY}$ and $\text{Corr}(Z,Y) = \rho_{YZ}$, the expected value of $\text{Corr}(X,Z)$ is simply equal to the product of $\rho_{XY} \times \rho_{YZ}$. To show this explicitly, note that ρ_{XY} is equal to

$$\rho_{XY} = \text{Corr}(X,Y) = \frac{\text{Cov}(X,Y)}{\sqrt{\text{Var}(X)\text{Var}(Y)}}$$

and that

$$\begin{aligned}\text{Cov}(X,Y) &= \text{Cov}(A_0 + A_1Y + \varepsilon_1, Y)\\ &= A_1\text{Var}(Y) + \text{Cov}(\varepsilon_1, Y)\\ &= A_1 \times \sigma_Y^2\end{aligned}$$

and

$$\begin{aligned}\text{Var}(X) &= \text{Var}(A_0 + A_1Y + \varepsilon_1)\\ &= A_1^2\text{Var}(Y) + \text{Var}(\varepsilon_1)\\ &= A_1^2\,\sigma_Y^2 + \eta_1^2\end{aligned}$$

Therefore, because $\text{Var}(Y) = \sigma_Y^2$, ρ_{XY} can be rewritten as

$$\rho_{XY} = \frac{A_1\sigma_Y}{\sqrt{(A_1^2\,\sigma_Y^2 + \eta_1^2)}} = \frac{A_1\sigma_Y}{\sqrt{\text{Var}(X)}}$$

In a similar manner, ρ_{YZ} can be rewritten as

$$\rho_{YZ} = \frac{B_1\sigma_Y}{\sqrt{(B_1^2\,\sigma_Y^2 + \eta_2^2)}} = \frac{B_1\sigma_Y}{\sqrt{\text{Var}(Z)}}$$

Now, note that

$$\text{Corr}(X,Z) = \frac{\text{Cov}(X,Z)}{\sqrt{\text{Var}(X),\,\text{Var}(Z)}}$$

and $\text{Cov}(X,Z)$ can be expanded as

$$\begin{aligned}\text{Cov}(X,Z) &= \text{Cov}(A_0 + A_1Y + \varepsilon_1,\, B_0 + B_1Y + \varepsilon_2)\\ &= \text{Cov}(A_1Y, B_1Y) + \text{Cov}(A_1Y, \varepsilon_2) +\\ &\quad \text{Cov}(B_1Y, \varepsilon_1) + \text{Cov}(\varepsilon_1, \varepsilon_2)\\ &= A_1B_1\text{Var}(Y)\\ &= A_1B_1\sigma_Y^2\end{aligned}$$

because the last three terms in the expansion have expectations of 0 under the previously stated assumptions. Hence,

$$\text{Corr}(X,Z) = \left[\frac{A_1\sigma_Y}{\sqrt{\text{Var}(X)}}\right] \times \left[\frac{B_1\sigma_Y}{\sqrt{\text{Var}(Z)}}\right] = \rho_{XY}\rho_{YZ}$$

Part A.2

An approximate F-test statistic for determining if the increase in the correlation coefficient is statistically significant can be developed as follows. Let $\mathbf{Y}$ represent the vector of averaged EM data, $\mathbf{X}$ the corresponding vector of ordinary DPPC conductivity calculations, and $\mathbf{W}$ the corresponding vector of optimized Dy-DPPC conductivity calculations. (All of the above mentioned data may be log-transformed; whether or not such a transformation is employed is irrelevant to this discussion.) Define $\text{Corr}(\mathbf{Y},\mathbf{X}) = r_1$ to be the calculated EM–DPPC correlation and $\text{Corr}(\mathbf{Y},\mathbf{W}) = r_2$ to be the optimized EM–Dy-DPPC correlation.

First, note that when we calculate the r_1 correlation, we are implicitly minimizing the sum of square error term in the following linear regression model:

$$\mathbf{Y} = \alpha_0 + \alpha_1(\mathbf{X})$$

Define SSE_1 to be the sum of square error estimate produced by this model (having $n - 2$ degrees of freedom). Additionally, when we optimize the EM–Dy-DPPC correlation estimate (r_2), we are also implicitly minimizing the sum of square error term in the following nonlinear regression model:

$$\mathbf{Y} = \phi_0 + \phi_1(\mathbf{W} \mid \beta_0, \beta_1)$$

where β_0 and β_1 represent the bounded logistic function parameters (which in turn define the value of δ in the Dy-DPPC equation). Define SSE_2 to be the sum of square error estimate produced by this model (having $n - 4$ degrees of freedom). Furthermore, note that the Dy-DPPC equation reduces to the ordinary DPPC equation whenever $\delta = 1$ (i.e., whenever β_0

and β_1 are defined to be arbitrarily large); hence, these two equations represent *nested* models (Bates and Watts, 1988, p. 103–104). Therefore, given a sample size of n, the following F score can be constructed:

$$F = [(SSE_1 - SSE_2)/2\ ]/[SSE_2/(n - 4)]$$

which can used as an approximate F-test statistic with 2 and $n - 4$ degrees of freedom. Note that this essentially represents an approximate test of (β_0, $\beta_1 \neq +\infty$), which is equivalent to testing for statistical significance in the correlation estimate improvement.

Part A.3

An approximate 95% confidence interval for each predicted EM–soil property correlation estimate can be constructed as follows. Let **x**, **y**, and **z** represent the observed data vectors from three stochastic random variables with finite mean and variance and let the variance of **y** be represented as s_Y^2. (Without loss of generality, let **x** represent EC_e data, **y** the $CalcEC_a$ data, and **z** averaged EM data.) Suppose again that both **x** and **z** are related to **y** in a linear manner; i.e.,

$$\mathbf{x} = \alpha_0 + \alpha_1(\mathbf{y}) + e_1,\ \mathrm{Var}(e_1) = m_1^2$$
$$\mathbf{z} = b_0 + b_1(\mathbf{y}) + e_2,\ \mathrm{Var}(e_2) = m_2^2$$

Then the following relationships hold (these follow directly from the derivations presented in Proof A.1):

$$\mathrm{Var}(\mathbf{x}) = \alpha_1^2 s_{\mathbf{Y}}^2 + m_1^2$$
$$\mathrm{Var}(\mathbf{z}) = b_1^2 s_{\mathbf{Y}}^2 + m_2^2$$
$$\mathrm{Cov}(\mathbf{x},\mathbf{y}) = \alpha_1 s_{\mathbf{Y}}^2$$
$$\mathrm{Cov}(\mathbf{y},\mathbf{z}) = b_1 s_{\mathbf{Y}}^2$$

and

$$\begin{aligned}\mathrm{Cov}(\mathbf{x},\mathbf{z}) &= \mathrm{Cov}(\alpha_1\mathbf{y},b_1\mathbf{y}) + \mathrm{Cov}(\alpha_1\mathbf{y},e_2) + \\ &\quad \mathrm{Cov}(b_1\mathbf{y},e_1) + \mathrm{Cov}(e_1,e_2) \\ &= \alpha_1 b_1 \mathrm{Var}(\mathbf{y}) + \mathrm{Cov}(e_1,e_2) \\ &= \alpha_1 b_1 s_{\mathbf{Y}}^2 + \sqrt{\mathrm{Var}(e_1)\mathrm{Var}(e_2)} \times \mathrm{Corr}(e_1,e_2) \\ &= \alpha_1 b_1 s_{\mathbf{Y}}^2 + m_1 m_2 \mathrm{Corr}(e_1,e_2)\end{aligned}$$

This is because the two middle covariance terms are constrained to be exactly equal to 0 by the regression model fitting procedure. Furthermore, because

$$\mathrm{Corr}(\mathbf{x},\mathbf{y}) = r_{\mathbf{XY}} = \frac{\alpha_1 s_{\mathbf{Y}}}{\sqrt{\alpha_1^2 s_{\mathbf{Y}}^2 + m_1^2}}$$

the following $r_{\mathbf{XY}}$ algebraic relationships hold

$$r_{\mathbf{XY}}^2 = \frac{\alpha_1^2 s_{\mathbf{Y}}^2}{(\alpha_1^2 s_{\mathbf{Y}}^2 + m_1^2)}$$
$$1 - r_{\mathbf{XY}}^2 = \frac{m_1^2}{(\alpha_1^2 s_{\mathbf{Y}}^2 + m_1^2)}$$
$$\sqrt{1 - r_{\mathbf{XY}}^2} = \frac{m_1}{\sqrt{\alpha_1^2 s_{\mathbf{Y}}^2 + m_1^2}}$$

Likewise,

$$\sqrt{1 - r_{\mathbf{YZ}}^2} = \frac{m_2}{\sqrt{b_1^2 s_{\mathbf{Y}}^2 + m_2^2}}$$

Therefore, the formula for Corr(**x**,**z**) may be derived from the Cov(**x**,**z**) equation as

$$r_{\mathbf{XZ}} = r_{\mathbf{XY}} r_{\mathbf{YZ}} + \left(\sqrt{1 - r_{\mathbf{XY}}^2}\ \sqrt{1 - r_{\mathbf{YZ}}^2}\right)\mathrm{Corr}(e_1,e_2)$$

This last formula is enlightening because it shows that the observed residual correlation estimate [Corr(e_1, e_2)] is simply the partial correlation coefficient between the **x** and **z** variables, after adjusting for the **y** variable. Additionally, because the distribution of the partial correlation coefficient is well known (i.e., see Graybill, 1976, Chapter 11), a 95% confidence interval can be immediately derived. Specifically, if $R_e = \mathrm{Corr}(e_1, e_2)$, then the transformed variable

$$T = \frac{R_e \sqrt{n - 3}}{\sqrt{1 - R_e^2}}$$

will follow a Student t distribution under the null hypothesis that $R_e = 0$. Hence, if $t_{0.975}$ is defined to be the 97.5% probability point of the Student t distribution with $n - 3$ degrees of freedom, a 95% confidence interval for the $r_{\mathbf{XY}}r_{\mathbf{YZ}}$ product correlation estimate can be calculated as

$$r_{\mathbf{XY}}r_{\mathbf{YZ}} \pm \left(\sqrt{1 - r_{\mathbf{XY}}^2}\ \sqrt{1 - r_{\mathbf{YZ}}^2}\right)\left(\frac{t_{0.975}}{\sqrt{n - 3 + t_{0.975}^2}}\right)$$

Notes:

1. The assumption of residual independence is intuitively equivalent to the assumption that the DPPC model is correctly specified. In situations where the DPPC model is seriously misspecified, significant residual correlation will generally be present. In turn, the observed $r_{\mathbf{XZ}}$ correlation estimate will appear to be considerably outside the $r_{\mathbf{XY}}r_{\mathbf{YZ}}$ confidence interval.
2. The above derivation also clearly depends on the assumption that the e_1 and e_2 residual errors are *spatially* independent. In practice, if this assumption is not correct, the derived 95% confidence intervals will underestimate the true 95% coverage probability. Because spatially correlated residuals are always of some concern, these confidence intervals should be interpreted cautiously.

ACKNOWLEDGMENTS

The authors appreciate the assistance of Robert LeMert and Nahid Vishteh for their help in collecting and analyzing the soil sample data associated with the Salinity Laboratory survey projects. The authors also acknowledge and thank the following people for assisting in the collection of and/or supplying data for the various survey projects discussed in this manuscript: Donald Ackley (Coachella Valley Water District), Steve Burch (Imperial Irrigation District), Cliff Landers (Soil and Water West), Murray Riddell (Genesis Environmental Limited), and Dr. Lorenz Sutherland (USDA-NRCS).

REFERENCES

Bates, D.M., and D.G. Watts. 1988. Nonlinear regression analysis and applications. John Wiley & Sons, New York.

Cook, P.G., G.R. Walker, G. Buselli, I. Potts, and A.R. Dodds. 1992. The application of electromagnetic techniques to groundwater recharge investigations. J. Hydrol. (Amsterdam) 130:201–229.

Corwin, D.L., M.L.K. Carrillo, P.J. Vaughan, J.D. Rhoades, and D.G.

Cone. 1999. Evaluation of a GIS-linked model of salt loading to groundwater. J. Environ. Qual. 28:471–480.
Corwin, D.L., S.R. Kaffka, J.D. Oster, J. Hopmans, Y. Mori, J.W. van Groenigen, C. van Kessel, and S.M. Lesch. 2003. Assessment and field-scale mapping of soil quality and hydrological characteristics of a saline-sodic soil. Geoderma (in press).
Corwin, D.L., and S.M. Lesch. 2003. Application of soil electrical conductivity to precision agriculture: Theory, principles, and guidelines. Agron. J. 95:(in press).
Corwin, D.L., J.D. Rhoades, and P.J. Vaughan. 1996. GIS applications to the basin-scale assessment of soil salinity and salt loading to ground water. p. 295–313. *In* D.L. Corwin, K. Loague, and T.R. Ellsworth (ed.) Application of GIS to the modeling of non-point source pollutants in the vadose zone. SSSA Spec. Publ. 48. SSSA, Madison, WI.
Doolittle, J.A., K.A. Dudduth, N.R. Kitchen, and S.J. Indorante. 1994. Estimating depths to clay pans using electromagnetic induction methods. J. Soil Water Conserv. 49:572–575.
Graybill, F.A. 1976. Theory and application of the linear model. Wadsworth Publ. Co., Belmont, CA.
Hendrickx, J.M.H., B. Baerends, Z.I. Raza, M. Sadig, and M.A. Chaudhry. 1992. Soil salinity assessment by electromagnetic induction of irrigated land. Soil Sci. Soc. Am. J. 56:1933–1941.
Hendrickx, J.M.H., and R.G. Kachanoski. 2002. Solute content and concentration—indirect measurement of solute concentration: Non-intrusive electromagnetic induction. *In* J.W. Dane and G.P. Topp (ed.) Methods of soil analysis. Part 4. SSSA Book Ser. 5. SSSA and ASA, Madison, WI.
Jaynes, D.B., T.S. Colvin, and J. Ambuel. 1995. Yield mapping by electromagnetic induction. p. 383–394. *In* P.C. Robert et al. (ed.) Site-specific management for agricultural systems. ASA, CSSA, and SSSA, Madison, WI.
Kachanoski, R.G., E.G. Gregorith, and I.J. van Wesenbeeck. 1988. Estimating spatial variations of soil water content using noncontacting electromagnetic inductive methods. Can. J. Soil Sci. 68: 715–722.
Kitchen, N.R., K.A. Sudduth, and S.T. Drummond. 1996. Mapping of sand deposition from 1993 midwest floods with electromagnetic induction measurements. J. Soil Water Conserv. 51:336–340.
Lesch, S.M., J. Herrero, and J.D. Rhoades. 1998. Monitoring for temporal changes in soil salinity using electromagnetic induction techniques. Soil Sci. Soc. Am. J. 62:232–242.
Lesch, S.M., J.D. Rhoades, and D.L. Corwin. 2000. ESAP-95 version 2.01R user manual and tutorial guide. Res. Rep. 146. George E. Brown, Jr., Salinity Lab, Riverside, CA.
Lesch, S.M., D.J. Strauss, and J.D. Rhoades. 1995a. Spatial prediction of soil salinity using electromagnetic induction techniques: I. Statistical prediction models: A comparison of multiple linear regression and cokriging. Water Resour. Res. 31:373–386.
Lesch, S.M., D.J. Strauss, and J.D. Rhoades. 1995b. Spatial prediction of soil salinity using electromagnetic induction techniques: II. An efficient spatial sampling algorithm suitable for multiple linear regression model identification and estimation. Water Resour. Res. 31:387–398.
McNeill, J.D. 1980. Electromagnetic terrain conductivity measurement at low induction numbers. Geonics Tech. Note TN-6. Geonics Limited, Mississauga, ON, Canada.
Rhoades, J.D. 1992. Instrumental field methods of salinity appraisal. p. 231–248. *In* G.C. Topp, W.D. Reynolds, and R.E. Green (ed.) Advances in measurement of soil physical properties: Bringing theory into practice. SSSA Spec. Publ. 30. SSSA, Madison, WI.
Rhoades, J.D. 1996a. New assessment technology for the diagnosis and control of salinity in irrigated lands. p. 1–9. *In* Proc. Int. Symp. on Dev. of Basic Technol. for Sustainable Agric. Under Saline Conditions, Tottori, Japan. 12 Dec. 1996. Tottori Univ., Tottori, Japan.
Rhoades, J.D. 1996b. Salinity: Electrical conductivity and total dissolved solids. p. 417–435. *In* D.L. Sparks et al. (ed.) Methods of soil analysis. Part 3. SSSA Book Ser. 5. SSSA and ASA, Madison, WI.
Rhoades, J.D., F. Chanduvi, and S.M. Lesch. 1999b. Soil salinity assessment: Methods and interpretation of electrical conductivity measurements. FAO Irrig. and Drain. Paper 57. FAO, Rome.
Rhoades, J.D., D.L. Corwin, and S.M. Lesch. 1999a. Geospatial measurements of soil electrical conductivity to assess soil salinity and diffuse salt loading from irrigation. p. 197–215. *In* D.L. Corwin, K. Loague, and T.R. Ellsworth (ed.) Assessment of non-point source pollution in the vadose zone. Geophysical Monogr. 108. Am. Geophysical Union, Washington, DC.
Rhoades, J.D., S.M. Lesch, R.D. LeMert, and W.J. Alves. 1997. Assessing irrigation/drainage/salinity management using spatially referenced salinity measurements. Agric. Water Manage. 35:147–165.
Rhoades, J.D., N.A. Manteghi, P.J. Shouse, and W.J. Alves. 1989. Soil electrical conductivity and soil salinity: New formulations and calibrations. Soil Sci. Soc. Am. J. 53:433–439.
SAS Institute. 1999. Base and stat software. Version 8.1. SAS Inst., Cary, NC.
Sheets, K.R., and J.M.H. Hendrickx. 1995. Non-invasive soil water content measurement using electromagnetic induction. Water Resour. Res. 31:2401–2409.
Slavich, P.G., and G.H. Petterson. 1990. Estimating average rootzone salinity from electromagnetic induction (EM-38) measurements. Aust. J. Soil Res. 28:453–463.
Suddeth, K.A., N.R. Kitchen, D.F. Huges, and S.T. Drummond. 1995. Electromagnetic induction sensing as an indicator of productivity on clay pan soils. p. 671–681. *In* P.G. Probert, R.I.H. Rust, and W.E. Larson (ed.) Proc. Int. Conf. of Site Specific Manage. for Agric. Syst., 2nd, Minneapolis, MN. ASA, CSSA, and SSSA, Madison, WI.
Triantafilis, J., A.I. Huckel, and A.B. McBratney. 1998. Estimating deep drainage on the field scale using a mobile EM sensing system and Sodium-SaLF. p. 61–64. *In* Proc. Australian Cotton Growers Res. Assoc. Conf., 9th, Broadbeach, QLD, Australia. 12–14 Aug. 1998. Australian Cotton Growers Res. Assoc., Broadbeach, QLD, Australia.
Williams, B.G., and G.C. Baker. 1982. An electromagnetic induction technique for reconnaissance surveys of soil salinity hazards. Aust. J. Soil Res. 20:107–118.
Williams, B.G., and D. Hoey. 1987. The use of electromagnetic induction to detect the spatial variability of the salt and clay contents of soils. Aust. J. Soil Res. 25:21–28.